NeuroImage: Clinical 4 (2014) 302–307

Contents lists available at ScienceDirect

NeuroImage: Clinical

journal homepage: www.elsevier.com/locate/ynicl

MRI texture heterogeneity in the optic nerve predicts visual recovery after acute optic neuritis☆

Yunyan Zhang [a,b,d,*], Luanne M. Metz [b,d], James N. Scott [a,b], Jessie Trufyn [b,d], Gordon H. Fick [c], Fiona Costello [b,d]

[a] Department of Radiology, University of Calgary, 3330 Hospital Dr NW, Calgary, Alberta T2N 4N1, Canada
[b] Department of Clinical Neurosciences, University of Calgary, 3330 Hospital Dr NW, Calgary, Alberta T2N 4N1, Canada
[c] Department of Community Health Sciences, University of Calgary, 3330 Hospital Dr NW, Calgary, Alberta T2N 4N1, Canada
[d] Hotchkiss Brain Institute, University of Calgary, 3330 Hospital Dr NW, Calgary, Alberta T2N 4N1, Canada

ARTICLE INFO

Article history:
Received 30 October 2013
Received in revised form 20 December 2013
Accepted 6 January 2014
Available online 14 January 2014

Keywords:
Acute tissue damage
MRI
Texture heterogeneity
Visual recovery
Prediction
Optic neuritis

ABSTRACT

Purpose: To test the feasibility of using multi-scale MRI texture analysis to assess optic nerve pathology and to investigate how visual recovery relates to the severity of acute tissue damage in the optic nerve in patients after optic neuritis (ON).
Materials and Methods: We recruited 25 patients with acute ON. Retinal nerve fiber layer (RNFL) thickness; MRI lesion length and enhancement; optic nerve area ratio; and multi-scale MRI texture analysis, a measure of structural integrity, were used to assess tissue damage at baseline, and at 6 and 12 months. The recovery in vision was defined as the functional outcome. Eight healthy subjects were imaged for control.
Results: We identified 25 lesions in the affected eyes (9 enhanced) and 5 in the clinically non-affected eyes (none enhanced). At baseline, we found that RNFL values were 20% thicker and lesion texture 14% more heterogeneous in the affected eyes than in the non-affected eyes, and lesion texture ratio of affected to non-affected eyes was greater in patients than in controls. In the affected eyes, visual acuity recovered significantly over 6 (18/23 patients) and 12 months (18/21 patients) when RNFL thickness and optic nerve area ratio decreased over time. Texture heterogeneity in the standard MRI of acute optic nerve lesions was the only measure that predicted functional recovery after ON.
Conclusions: Tissue heterogeneity may be a potential measure of functional outcome in ON patients and advanced analysis of the texture in standard MRI could provide insights into mechanisms of injury and recovery in patients with similar disorders.

1. Introduction

Functional recovery varies in patients with multiple sclerosis (MS) following acute inflammation (Hirst et al., 2012) and is difficult to predict. As an acute inflammatory episode affecting the optic nerve and a frequent initial presentation of MS (Balcer, 2006), optic neuritis (ON) is often used as a model to study the relationship between structure and function; both can be measured independently (Jenkins et al., 2009). The ability to predict functional recovery at symptom onset may have potential implications in the long-term treatment of MS.

Currently whether and how optic nerve damage relates to visual recovery after acute ON is not fully understood. Some report that shorter enhancing lesions in magnetic resonance imaging (MRI) (Hickman et al., 2004a) and slower loss of retinal nerve fiber layer (RNFL) thickness in early ON (Costello et al., 2006) correlate to better visual outcome. But others claim that acute MRI lesions do not consistently predict visual recovery (Hickman et al., 2004a; Kupersmith et al., 2011), and that visual acuity at month 12 does not correlate with acute tissue injury in ON measured by visual evoked potential, RNFL, MRI lesion length, or diffusion tensor imaging (DTI) (Jenkins et al., 2010).

Advanced analysis of the severity of tissue damage may help us clarify the interactions between structure and function. MRI texture analysis is a quantitative approach that evaluates inter-voxel relationships in an image and has shown great potential to detect subtle structural changes following acute inflammation (Kassner and Thornhill, 2010; Zhang, 2012). For example, using a local spatial frequency-based analysis technique, polar Stockwell transform (PST), investigators found that MRI texture analysis not only correlates with the type of pathological damage in postmortem MS brain, but also in vivo, it differentiates acute lesions from chronic lesions (Zhang et al., 2009) and distinguishes acute lesions that persist from those that recover 5 to 8 months earlier than visual perception in MS (Zhang et al., 2011). Using a similar

* Corresponding author at: 183 Heritage Medical Research Building, 3330 Hospital Dr NW, Calgary AB T2N 4N1, Canada. Tel.: +1 403 220 2909; fax: +1 403 283 8731.
E-mail address: yunyzhan@ucalgary.ca (Y. Zhang).

2213-1582/$ – see front matter © 2014 The Authors. Published by Elsevier Inc. All rights reserved.
http://dx.doi.org/10.1016/j.nicl.2014.01.003

approach, another group found that acute lesion texture in baseline MRI predicted disability progression over 2 years in MS patients (Loizou et al., 2010).

Our goal of this study was to evaluate prospectively how visual recovery relates to the severity of acute tissue damage in the optic nerve assessed by PST texture analysis, and other structural measures including MRI enhancing and non-enhancing lesion length, optic nerve area, and RNFL thickness assessed by optical coherence tomography (OCT).

2. Material and methods

2.1. Participants

Twenty-five patients with acute ON in the context of relapsing–remitting MS (Polman et al., 2005) or clinically isolated syndrome (CIS) were recruited within two weeks of symptom onset. Participants with any other neurological or ophthalmologic diseases were excluded. Ophthalmic, MRI, and OCT assessments were performed at baseline, and at 6 and 12 months thereafter. Eight age- and gender-matched healthy subjects were imaged for control. This study was approved by the Institutional Health Research Ethics Board, and written informed consent was obtained from each participant. All clinical investigations were conducted according to the Declaration of Helsinski.

2.2. Ophthalmic Assessment

High-contrast visual acuity was assessed using the Early Treatment Diabetic Retinopathy Study (ETDRS) chart at 4 m. Participants wore contact lenses or glasses if applicable and were instructed to read the letters by each eye. The number of letters identified out of 70 was considered the best-corrected visual acuity, recorded as logMAR (logarithm of the minimum angle of resolution) (Ferris et al., 1982). Higher logMAR values represent poorer vision, and the worst vision score of 1.5 was assigned to the participants who recognized no letters but perceived hand motion, light perception, or neither.

2.3. OCT Testing

Peripapillary images of RNFL were acquired using OCT (Stratus version 3; Carl Zeiss Meditec, Dublin, USA). After mydriasis with 1% tropicamide, three retinal scans were conducted circularly with a diameter of 3.4 mm, from which the RNFL thickness at 256 points of the circumference was recorded per scan. The mean RNFL value in each eye was obtained using an automatic algorithm as reported previously (Costello et al., 2006).

2.4. MRI Protocol

All participants were imaged within 4 weeks of ON at a 3 T scanner (GE Signa, WI, USA) using optimized optic nerve protocols. These included: coronal short tau inversion recovery (STIR) sequence [repetition time (TR) = 4500 ms, echo time (TE) = 46 ms, inversion recovery = 195 ms]; coronal spin echo T1-weighted pre- and 5-min post-contrast fat-saturated sequences [TR = 500 ms, TE = 15 ms], with identical settings for field of view (18×18 cm^2), matrix size (512×512), and slice thickness (4 mm). Participants were instructed to limit movement and close eyes during imaging to minimize artifacts. Control subjects were imaged one time only without contrast.

2.5. Anatomical MRI Analysis

Lesion length was evaluated on the coronal STIR images as slice thickness multiplied by the number of slices showing signal abnormality. Also in STIR MRI, cross-sectional area of the optic nerve was quantified using a semi-automatic region-growing algorithm (Osirix for Mac), and the averaged area from 3 consecutive slices central, anterior, and posterior to the lesion was used as the final value for the optic nerve. In the non-ON or control eyes, optic nerve area was obtained by averaging areas from 3 equivalent MRI locations of the optic nerve as those set for the ON eyes. Then, the ratio of affected (ON) to clinically non-affected (non-ON) optic nerve area in patients, right to left optic nerve area ratio in controls, was computed to account for inter-subject variability, a suggested approach in optic nerve studies (Henderson et al., 2010; Klistorner et al., 2008). Gadolinium-enhancing activity was evaluated on the fat-saturated post-contrast T1 MRI in all but 2 participants who declined contrast injection, by two MRI neuroradiologists (YZ & JNS, both with over 10 years of experience). The entire image analysis for one participant took approximately half an hour, including the semi-automatic measurements (YZ, 11 years of experience).

2.6. Multi-scale MRI Texture Analysis

The coronal STIR image showing the largest cross-sectional area of the lesion was used for texture analysis. This MRI contrast had the ability to capture the inclusive changes raised by ON lesions that also lasted longer in this imaging sequence. As reported previously (Zhang et al., 2009; Zhu et al., 2004), fast Fourier transform was initially conducted to obtain the total frequency content in the image and then for each frequency, its spectral amplitude at individual voxel locations was determined by performing inverse Fourier transform. Eventually, a multi-scale texture spectrum at each voxel was derived ranging from coarse to fine texture (Fig. 1). Each of these steps can be done using open source software such as ImageJ (NIH, USA). In this study, the analysis was centered at the optic nerves with an area of 300×300 voxels, and a high spectral resolution of 0.009 hertz/mm was achieved for detailed structural evaluation.

Based on the dissimilarity in texture spectra between lesion and reference voxels in the white matter, texture heterogeneity maps were calculated (see Fig. 1). This was based on the theory of dot product in mathematics (Spiegel et al., 2009), which computed the phase angle between texture spectra that were treated as multi-dimension vectors. As the distribution of texture spectrum reflects the local pattern of image voxels that in turn relates to the organization of tissue microstructure, greater texture heterogeneity represents greater loss of tissue regularity. Lesion texture of the optic nerve was extracted from the heterogeneity maps by applying corresponding lesion masks that were derived from the measurement of optic nerve area in STIR MRI. Similarly, control nerve texture was obtained based on the masks of control nerve area that corresponded to the center of ON lesions. Again, the ratio of ON to non-ON nerve texture (right to left in controls) was used to compare between cohorts and timepoints. The reliability of our assessing methods was tested using the left and right eyes in control subjects.

2.7. Statistical Analysis

Two-variable comparisons were done using Student's *t*-test, and mixed-effect modeling was used to explore longitudinal changes. Functional outcome was defined as the recovery in logMAR over time from baseline. The relationship between baseline measures and functional outcome was assessed, firstly by univariate regression, and then by multiple regression on all variables showing importance ($p \leq 0.1$) individually, using age and non-ON eye visual acuity as covariates. Finally, all baseline structural measures were included in the model to identify independent predictors of functional outcome. All analyses were conducted using Stata 12 (StataCorp, College Station, TX, USA); $p \leq 0.05$ was set as significance. Subjects with incomplete datasets were excluded from analyses.

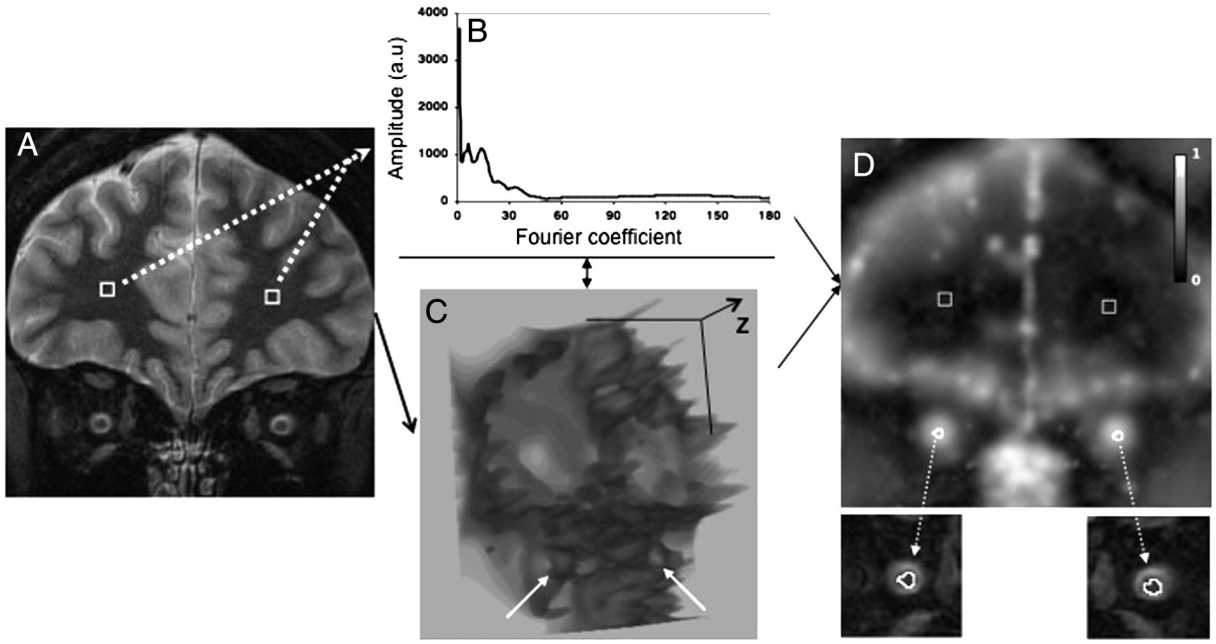

Fig. 1. A demonstration of our texture analysis method. In the coronal STIR MR image (A), two reference regions (squares, 10 × 10 voxel each) were chosen symmetrically in the normal appearing white matter (NAWM) of bi-hemispheres. Using the polar Stockwell transform, multi-scale texture spectra of the NAWM (B) and the whole image (C) were computed, one spectrum per voxel that forms a spectral stack from all voxels in C. Calculating the spectral difference between B and C gives rise to the texture heterogeneity map for image A (D), wherein the texture of optic nerves was highlighted (irregular outlines in D) by the regions of interest segmented from the anatomical MRI (small images below D).

3. Results

3.1. Demographic and Clinical Characteristics

Of the 25 participants, 16 of them had ON in the left eye (OS), 9 in the right eye (OD), and 4 in the fellow eye prior to (3 subjects) or during the study (1 subject). The mean (range) age of all subjects was 33 (22–50) years; EDSS score was 1.2 (0–3) and disease duration was 4 (0–13) years in MS subjects. Twenty-three participants completed month-6 follow-up and 21 completed month-12 follow-up. Two subjects (1 MS; 1 CIS) received high-dose corticosteroid to treat acute ON; 6 MS subjects were using disease-modifying therapies (3 on glatiramer acetate; 3 on interferon beta); and the degree of visual recovery was not different between MS and CIS patients (Table 1).

3.2. Lesion Characteristics

There were 22 focal hyperintense lesions in the ON eyes (11 MS; 11 CIS) and 5 in the non-ON eyes of MS patients, and there was subtle signal abnormality in the other 3 ON eyes (2 MS; 1 CIS). Nine focal lesions enhanced, all in the ON eyes (5 MS; 4 CIS). No lesions were identified in the non-ON eyes of CIS patients, and no abnormality was found in any of the control subjects.

3.3. Baseline Structural and Functional Outcomes

Within subjects, visual acuity was 0.50-unit worse ($p < 0.001$); RNFL was 20% thicker ($p < 0.001$); and MRI texture was 14% ($p = 0.10$) coarser in the ON eyes than in the non-ON eyes (Fig. 2). In patients, optic nerve texture ratio was 24% greater ($p = 0.04$) and optic nerve area ratio was 7% larger ($p = 0.39$) than in controls. No difference was detected in any measurements between MS and CIS participants (Table 2), or between two eyes of control subjects including MRI texture analysis ($p = 0.28$).

3.4. Longitudinal Structural and Functional Outcomes

Compared to baseline, visual acuity improved in most subjects over time ($p < 0.01$), and no subject experienced visual worsening at one year. In particular, 18/23 (78%) participants showed recovery over 6 months, and 18/21 (86%) over 12 months; at both follow-ups, visual difference between ON and non-ON eyes was also resolved ($p = 0.91$

Table 1
Demographic and visual outcomes of patients with acute optic neuritis.

Patient ID	ON	Diagnosis	Visual recovery in logMAR	
			6 M vs baseline	12 M vs baseline
1	OD	MS	−0.5	−0.4
2	OS	CIS	0	0
3	OS	CIS	−1.6	−1.7
4	OD	CIS	−0.2	−0.3
5	OD	MS	0	−0.1
6	OS	MS	−0.3	−0.3
7	OD	CIS	0.1	−0.1
8	OS	CIS	−1.4	−1.4
9	OS	MS	−1.4	−1.1
10	OS*	MS	−0.7	−0.8
11	OD*	MS	−1.6	−1.5
12	OS	MS	−0.1	−0.3
13	OS	CIS	−0.1	0
14	OD*	MS	−0.7	−0.7
15	OS	CIS	−0.2	−0.2
16	OS	CIS	−0.1	0
17	OS	CIS	−0.4	−0.2
18	OS*	MS	−0.5	−0.5
19	OD	MS	−0.1	−0.1
20	OS	MS	−0.8	−0.8
21	OD	MS	−0.9	−0.8

Abbreviations: ON: optic neuritis; OD: right eye; OS: left eye; MS: multiple sclerosis; CIS: clinically isolated syndrome; LogMAR: logarithm of the minimum angle of resolution; M: month.
Note: All the listed patients here had complete datasets; those who had non-ON eye affected* prior to (# 10, 11, and 14) or during (#18) the study were excluded from ratio calculations.

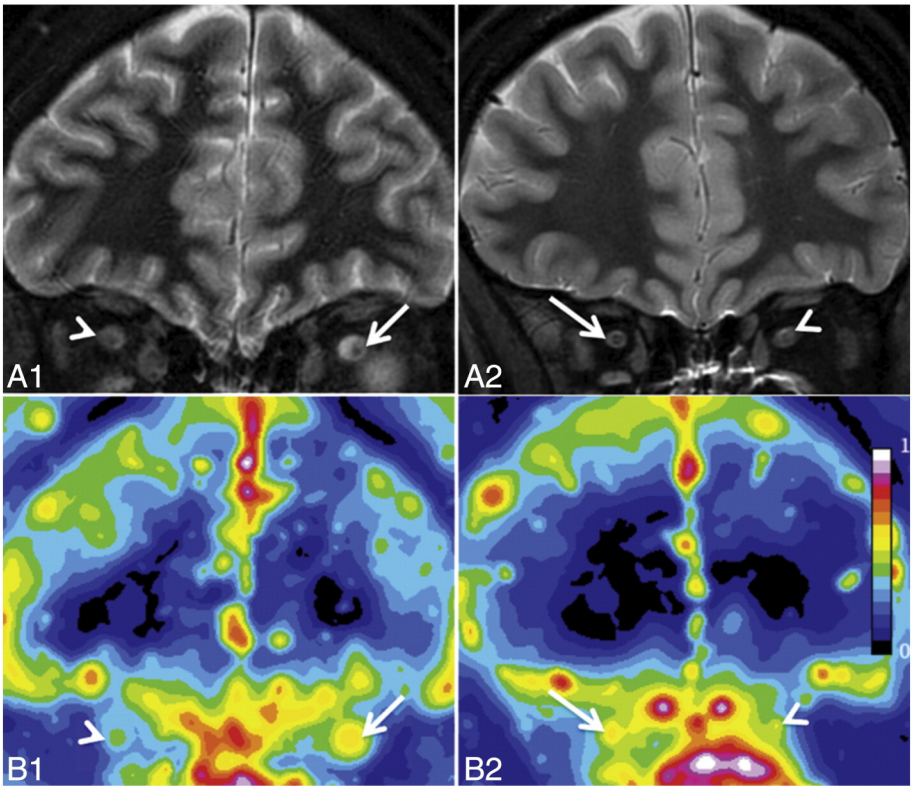

Fig. 2. Baseline MR images from two participants with acute optic neuritis showing different degrees of texture heterogeneity and visual recovery. The first subject (left column) shows a hyperintense lesion on STIR MRI (A1) in the left eye (arrows), with increased MRI texture heterogeneity (0.50 unit, yellow-red in B1) compared to the other eye (0.39 unit, green at arrow head in B1), and 12-month visual recovery of 0.8 logMAR unit. The other subject (right column) shows subtle abnormality in the right eye (arrow, A2), but with greater heterogeneity in MRI texture at baseline (0.62 unit, yellow–red in B2) and less visual recovery (0.1 logMAR unit). The control eye texture of this subject was 0.51 unit (green–yellow, arrow head in B2).

and 0.54). The change in lesion texture ratio was not significant ($p = 0.20$) but it followed a similar recovery pattern to that of visual function. RNFL thickness decreased at month 6 ($p < 0.01$) yet did not change significantly (3%) between 6 and 12 months in ON eyes and remained stable in non-ON eyes. Over 12 months, there was a 14% reduction in the optic nerve area ratio ($p = 0.03$) in ON patients, but no change in STIR lesion length ($p = 0.99$; Table 3).

Table 2
Baseline measures in optic neuritis eyes of patients with multiple sclerosis or clinically isolated syndrome and in control eyes.

	Outcome	Mean (stderr)	*p* value
MS ($n = 12$)	LogMAR	0.59 (0.15)	<0.001
	RNFL (micron)	122.80 (9.20)	0.03
	Texture value (a.u)	0.48 (0.03)	0.27
	Texture ratio	1.19 (0.10)	N/A
	Area ratio	1.14 (0.05)	N/A
	T2 lesion length (mm)	12.09 (1.26)	0.30
	Gd lesion length (mm)	9.17 (0.86)	N/A
CIS ($n = 9$)			
	LogMAR	0.46 (0.20)	0.03
	RNFL (micron)	121.89 (6.36)	0.01
	Texture value (a.u)	0.50 (0.05)	0.07
	Texture ratio	1.19 (0.10)	N/A
	Area ratio	1.08 (0.05)	N/A
	T2 lesion length (mm)	15.38 (2.00)	N/A
	Gd lesion length (mm)	9.00 (0.94)	N/A
Control ($n = 8$)			
	Texture ratio	0.93 (0.05)	0.04*
	Area ratio	1.05 (0.08)	0.39*

Abbreviations: ON: optic neuritis; MS: multiple sclerosis; CIS: clinically isolated syndrome; Gd: gadolinium; RNFL: retinal nerve fiber layer; logMAR: logarithm of the minimum angle of resolution; and a.u: arbitrary unit.
Note: *P* values with * indicate differences between ON patients and controls, otherwise between ON and non-ON eyes of the patients. Any subjects who had non-ON eye affected previously were excluded from texture and area ratio calculations.

3.5. Baseline Lesion Texture Heterogeneity Predicted Visual Recovery After ON

Baseline lesion texture independently correlated with the extent of visual recovery over 6 ($r = 0.49$, $p = 0.03$) and 12 months ($r = 0.50$, $p = 0.02$) in ON eyes (Fig. 3). Specifically, one unit decrease in lesion texture was related to 2 unit improvement in visual acuity (approximately 2 lines on the eye chart). No other MRI or ophthalmic variables at baseline correlated with visual recovery over 6 or 12 months, either individually or in combination with adjustment for age and non-ON eye visual acuity (Table 4). No month 6 variable correlated with visual recovery between 6 and 12 months.

4. Discussion

In this prospective study, we demonstrate that the severity of acute tissue damage in the optic nerve, as determined by MRI texture heterogeneity, predicts the degree of visual recovery in MS and CIS patients. As a potentially new measure of subtle pathological changes, PST texture heterogeneity outperforms several recognized structural metrics including RNFL, optic nerve area, and lesion length and activity.

PST texture analysis measures the regularity of tissue structure reflected by the patterns of image intensity but determined by the biophysical property of tissue microstructure. Consequently, pathological processes that involve remodeling of biological structure should lead to changes in the distribution pattern of MRI signal intensity and hence MRI texture (Yu et al., 2004). What makes it different from many other texture analysis methods is the ability of PST to detect tissue changes in both fine and coarse texture spectrum (ranging from sub-

Table 3
Longitudinal outcomes in the structure and function of optic neuritis eyes.

	Baseline	6 months	12 months	12-month change
	Mean (Stderr)	Mean (Stderr)	Mean (Stderr)	*p* value
ON logMAR	0.53 (0.11)	**−0.01 (0.03)**	**−0.01 (0.04)**	**<0.01**
Texture ratio	1.15 (0.08)	1.12 (0.04)	1.17 (0.05)	NS
RNFL (micron)	120.95 (5.65)	**92.52 (3.56)**	**86.50 (3.69)**	**<0.01**
Area ratio	1.11 (0.04)	1.03 (0.03)	**0.99 (0.04)**	**0.03**
T2 lesion length (mm)	13.21 (1.15)	13.17 (1.08)	13.29 (1.10)	NS
Gd lesion length (mm)	10.29 (0.41)	8*	/	N/A
Non-ON logMAR	−0.01 (0.03)	−0.02 (0.03)	−0.04 (0.04)	NS

Abbreviations: ON: optic neuritis; Gd: gadolinium; RNFL: retinal nerve fiber layer; logMAR: logarithm of the minimum angle of resolution; Stderr: standard error; NS: not significant; N/A: not applicable.
Note: Measures in bold reflect significant differences as compared to baseline; *p* values indicate levels of difference between month 12 and baseline measures. *: one lesion only.

millimeter to sub-centimeter scales in this study), suggesting enhanced sensitivity. Indeed, postmortem analysis in T2 MRI confirms that PST texture heterogeneity strongly correlates with the density of myelin stained by luxol fast blue, and at a lesser extent, the axonal density and inflammatory in MS brain (Zhang et al., 2013). Thus, in the current study, greater texture heterogeneity indicates more severe pathological damage in the optic nerve that relates to less recovery in vision.

Except MRI texture heterogeneity, we did not find significant correlations between other structural measures and visual recovery in this study. Post-acute measures of RNFL thickness have shown robust correlations with various visual outcomes in ON and MS patients (Cettomai et al., 2010; Costello et al., 2006; Fisher et al., 2006; Talman et al., 2010; Trip et al., 2005; Villoslada et al., 2012). Acutely, however, increased RNFL values, owing to optic disc swelling, may not correlate with the severity of tissue damage or visual dysfunction (Kupersmith et al., 2011). Similarly, acute enlargement of optic nerve area represents transient edema of the nerve in MRI (Hickman et al., 2004b). Although lesion length and enhancing activity both reflect the burden of inflammation, their correlation with clinical outcome is inconsistent in ON patients (Hickman et al., 2004a; Kupersmith et al., 2011).

We found that dominant recovery in vision occurred within 6 months of ON in our patients, consistent with prior observations (Brusa et al., 2001; Henderson et al., 2011; Smith et al., 2011). In this study, we aimed at the ON patients commonly seen at the daily clinic, in the context of either MS or CIS, to represent a general sample. Given a baseline logMAR of 0.53 in this group, regaining normal vision at month 6 suggests profound visual recovery. Over this period, both RNFL thickness and optical nerve area reduced significantly. Reportedly the rapid early decline in these metrics indicates resolution of acute inflammation, but not tissue atrophy (Hickman et al., 2004b; Kupersmith et al., 2011). And this recovering process, together with active remyelination evidenced to occur between 3 and 6 months of ON (Brusa et al., 2001; Klistorner et al., 2010), likely promotes visual recovery.

Chronic demyelination and axonal loss (Klistorner et al., 2008) however often overshadow the weakening process of remyelination (Brusa et al., 2001) over time, which may ultimately compromise functional repair (Brusa et al., 1999, 2001) and has also contributed to the persistence of lesion length and texture heterogeneity in this cohort. Additionally, there was up to a 30-day delay for the patients to have MRI after onset. Arguably, the most active phases of inflammation identified as enhancing lesions in the ON have been missed in some patients, which likely also contributed to the insignificant outcomes. Indeed, previous analysis found significant texture changes in only 12 acute brain lesions in the T2 MRI of MS patients (Zhang et al., 2009). In the future, we seek to confirm the current results in large-sample studies and to verify the relationship between acute inflammation, tissue heterogeneity, and functional recovery.

There are few structure integrity studies in the literature, mostly using DTI; and often, with disparate results. Some researchers demonstrate the potential of axial diffusivity 3 to 6 months after ON (Naismith et al., 2009, 2012) whereas others support baseline functional MRI but not DTI (Jenkins et al., 2010) to predict visual function. While the role of neuroplasticity is critical, the lack of difference between MS and CIS outcomes in this study supports the significance of the severity of acute tissue damage to functional repair. By analyzing the local pattern of signal intensity to infer tissue integrity, PST texture analysis is conceptually different from DTI, an advanced image acquisition-based

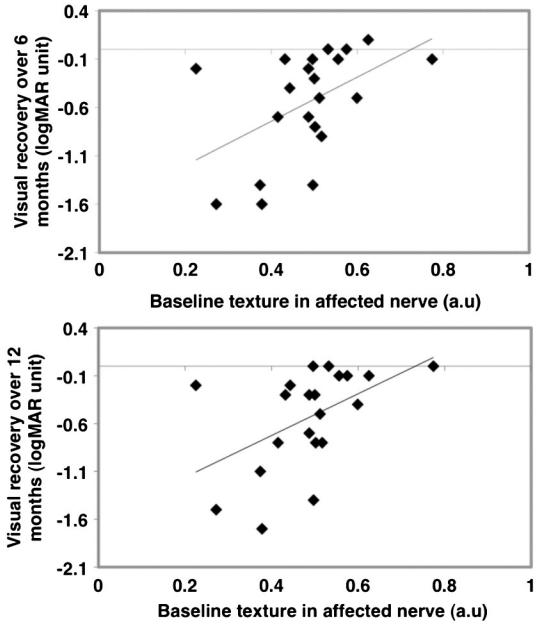

Fig. 3. Baseline MRI texture heterogeneity in the affected eyes of the optic neuritis patients predicts visual recovery over 6 and 12 months. Larger intercept in logMAR indicates greater change: below zero means recovery; above zero means worsening; and zero represents no change.

Table 4
The relationship between baseline measurements and visual recovery over 6 and 12 months in the optic neuritis eyes.

	6-month recovery		12-month recovery	
	r	*p*	*r*	*p*
Texture (a.u)	0.49	0.03	0.50	0.02
RNFL (micron)	0.05	0.82	0.05	0.85
Nerve Area ratio	−0.21	0.36	−0.18	0.46
T2 lesion length (mm)	−0.16	0.51	−0.20	0.44
Gd lesion length (mm)	0.02	0.95	0.03	0.92
Age (year)	0.03	0.91	0.11	0.64
Disease duration (year)	−0.06	0.81	−0.03	0.89
Non-ON logMAR	−0.09	0.75	−0.05	0.82

Abbreviations: ON: optic neuritis; Gd: gadolinium; RNFL: retinal nerve fiber layer; logMAR: logarithm of the minimum angle of resolution; a.u: arbitrary unit.

technique that measures the extent of random movement of water molecules in a tissue. Using clinical MRI that is easy to standardize and less susceptible to the small size and mobility of optic nerve, our results suggest that PST-measured structure heterogeneity may become a useful index of functional recovery in routine patient care.

We note some limitations in this study. First, our sample size is rather small limiting broad conclusions. In addition, we focused on the optic nerve, not other levels of visual hierarchy, yet this approach provided us a unique opportunity to examine structure and function independently. In texture analysis, we targeted the epicenter of optic nerve lesions. While this excluded peripheral pathology, our focus on the lesion core is consistent with the hallmark of MS pathology, multi-focal plaques (Lassmann et al., 1994). Further, we used high-contrast letter acuity to assess visual function. This conventional test of spatial visual perception has limited sensitivity (Fisher et al., 2006) and may have underestimated the visual deficit in our patients, although this measure shows promise in several studies of ON (Jenkins et al., 2010; Kolbe et al., 2009) and allowed us to demonstrate proof-of-concept evidence in this study. In future prospective investigations, we aim to validate our data by comparing with DTI and including comprehensive assessments of vision such as low-contrast letter acuity, contrast sensitivity, color vision, and mean deviation.

5. Conclusions

In this prospective study, we show that greater structural heterogeneity predicts less functional recovery in patients with acute ON. As an image post-processing technique, PST texture analysis is embeddable to standard MRI. By providing quantitative metrics of tissue injury and functional repair in a reasonable time window, this method may help enhance our patient care abilities in both diagnosis and treatment. Besides MS and CIS, this approach should benefit the patients with several other similar disorders.

Acknowledgments

The authors thank the Multiple Sclerosis Society of Canada for funding this study (FC) and the patient and healthy volunteers for participating in the research. Zhang Y receives research support from the Multiple Sclerosis Society of Canada and the Natural Sciences and Engineering Council of Canada. Metz LM receives research support from Multiple Sclerosis Scientific Research Foundation, Canada. Scott JN reports no disclosures. Trufyn J reports no disclosures. Fick GH reports no disclosures.

References

Balcer, L.J., 2006. Clinical practice. Optic neuritis. N. Engl. J. Med. 354 (12), 1273–1280.
Brusa, A., Jones, S.J., Kapoor, R., Miller, D.H., Plant, G.T., 1999. Long-term recovery and fellow eye deterioration after optic neuritis, determined by serial visual evoked potentials. J. Neurol. 246 (9), 776–782.
Brusa, A., Jones, S.J., Plant, G.T., 2001. Long-term remyelination after optic neuritis: a 2-year visual evoked potential and psychophysical serial study. Brain 124 (Pt 3), 468–479.
Cettomai, D., Hiremath, G., Ratchford, J., et al., 2010. Associations between retinal nerve fiber layer abnormalities and optic nerve examination. Neurology 75 (15), 1318–1325.
Costello, F., Coupland, S., Hodge, W., et al., 2006. Quantifying axonal loss after optic neuritis with optical coherence tomography. Ann. Neurol. 59 (6), 963–969.
Ferris III, F.L., Kassoff, A., Bresnick, G.H., Bailey, I., 1982. New visual acuity charts for clinical research. Am J. Ophthalmol. 94 (1), 91–96.
Fisher, J.B., Jacobs, D.A., Markowitz, C.E., et al., 2006. Relation of visual function to retinal nerve fiber layer thickness in multiple sclerosis. Ophthalmology 113 (2), 324–332.
Henderson, A.P., Altmann, D.R., Trip, A.S., et al., 2010. A serial study of retinal changes following optic neuritis with sample size estimates for acute neuroprotection trials. Brain 133 (9), 2592–2602.
Henderson, A.P., Altmann, D.R., Trip, S.A., et al., 2011. Early factors associated with axonal loss after optic neuritis. Ann. Neurol. 70 (6), 955–963.
Hickman, S.J., Toosy, A.T., Miszkiel, K.A., et al., 2004a. Visual recovery following acute optic neuritis—a clinical, electrophysiological and magnetic resonance imaging study. J. Neurol. 251 (8), 996–1005.
Hickman, S.J., Toosy, A.T., Jones, S.J., et al., 2004b. A serial MRI study following optic nerve mean area in acute optic neuritis. Brain 127 (Pt 11), 2498–2505.
Hirst, C.L., Ingram, G., Pickersgill, T.P., Robertson, N.P., 2012. Temporal evolution of remission following multiple sclerosis relapse and predictors of outcome. Mult. Scler. 18 (8), 1152–1158.
Jenkins, T., Ciccarelli, O., Toosy, A., et al., 2009. Dissecting structure–function interactions in acute optic neuritis to investigate neuroplasticity. Hum. Brain Mapp. 31 (2), 276–286.
Jenkins, T.M., Toosy, A.T., Ciccarelli, O., et al., 2010. Neuroplasticity predicts outcome of optic neuritis independent of tissue damage. Ann. Neurol. 67 (1), 99–113.
Kassner, A., Thornhill, R.E., 2010. Texture analysis: a review of neurologic MR imaging applications. AJNR Am. J. Neuroradiol. 31 (5), 809–816.
Klistorner, A., Arvind, H., Nguyen, T., et al., 2008. Axonal loss and myelin in early ON loss in postacute optic neuritis. Ann. Neurol. 64 (3), 325–331.
Klistorner, A., Arvind, H., Garrick, R., Yiannikas, C., Paine, M., Graham, S.L., 2010. Remyelination of optic nerve lesions: spatial and temporal factors. Mult. Scler. 16 (7), 786–795.
Kolbe, S., Chapman, C., Nguyen, T., et al., 2009. Optic nerve diffusion changes and atrophy jointly predict visual dysfunction after optic neuritis. Neuroimage 45 (3), 679–686.
Kupersmith, M.J., Mandel, G., Anderson, S., Meltzer, D.E., Kardon, R., 2011. Baseline, one and three month changes in the peripapillary retinal nerve fiber layer in acute optic neuritis: relation to baseline vision and MRI. J. Neurol. Sci. 308 (1–2), 117–123.
Lassmann, H., Suchanek, G., Ozawa, K., 1994. Histopathology and the blood-cerebrospinal fluid barrier in multiple sclerosis. Ann. Neurol. 36 (Suppl.), S42–S46.
Loizou, C.P., Murray, V., Pattichis, M.S., Seimenis, I., Pantziaris, M., Pattichis, C.S., 2010. Multiscale amplitude-modulation frequency-modulation (AM-FM) texture analysis of multiple sclerosis in brain MRI images. IEEE Trans. Inf. Technol. Biomed. 15 (1), 119–129.
Naismith, R.T., Xu, J., Tutlam, N.T., et al., 2009. Disability in optic neuritis correlates with diffusion tensor-derived directional diffusivities. Neurology 72 (7), 589–594.
Naismith, R.T., Xu, J., Tutlam, N.T., et al., 2012. Diffusion tensor imaging in acute optic neuropathies: predictor of clinical outcomes. Arch. Neurol. 69 (1), 65–71.
Polman, C.H., Reingold, S.C., Edan, G., et al., 2005. Diagnostic criteria for multiple sclerosis: 2005 revisions to the "McDonald Criteria". Ann. Neurol. 58 (6), 840–846.
Smith, S.A., Williams, Z.R., Ratchford, J.N., et al., 2011. Diffusion tensor imaging of the optic nerve in multiple sclerosis: association with retinal damage and visual disability. AJNR Am. J. Neuroradiol. 32 (9), 1662–1668.
Spiegel, M.R., Lipschutz, S., Spellman, D., 2009. Schaum's Outlines of Vector Analysis, 2nd ed. McGraw Hill.
Talman, L.S., Bisker, E.R., Sackel, D.J., et al., 2010. Longitudinal study of vision and retinal nerve fiber layer thickness in multiple sclerosis. Ann. Neurol. 67 (6), 749–760.
Trip, S.A., Schlottmann, P.G., Jones, S.J., et al., 2005. Retinal nerve fiber layer axonal loss and visual dysfunction in optic neuritis. Ann. Neurol. 58 (3), 383–391.
Villoslada, P., Cuneo, A., Gelfand, J., Hauser, S.L., Green, A., 2012. Color vision is strongly associated with retinal thinning in multiple sclerosis. Mult. Scler. 18 (7), 991–999.
Yu, O., Steibel, J., Mauss, Y., et al., 2004. Remyelination assessment by MRI texture analysis in a cuprizone mouse model. Magn. Reson. Imaging 22 (8), 1139–1144.
Zhang, Y., 2012. MRI texture analysis in multiple sclerosis. Int J Biomed Imaging. http://dx.doi.org/10.1155/2012/762804.
Zhang, Y., Zhu, H., Mitchell, J.R., Costello, F., Metz, L.M., 2009. T2 MRI texture analysis is a sensitive measure of tissue injury and recovery resulting from acute inflammatory lesions in multiple sclerosis. Neuroimage 47 (1), 107–111.
Zhang, Y., Traboulsee, A., Zhao, Y., Metz, L.M., Li, D.K., 2011. Texture analysis differentiates persistent and transient T1 black holes at acute onset in multiple sclerosis: a preliminary study. Mult. Scler. 17 (5), 532–540.
Zhang, Y., Moore, G.R., Laule, C., et al., 2013. Pathological correlates of MRI texture heterogeneity in multiple sclerosis. Ann. Neurol. 74 (1), 91–99.
Zhu, H., Zhang, Y., Wei, X., Metz, L.M., Mitchell, J.R., 2004. MR multi-spectral texture analysis using space-frequency information. In: Valafar, F., Valafar, H. (Eds.), Proceedings of the International Conference on Mathematics and Engineering Techniques in Medicine and Biological Sciences (METMBS), June 21–24, Las Vegas, Nevada, USA, pp. 173–179.